Sensors & Transducers

Detection and Discrimination Methods of Sub-ppm Nitrogen Dioxide (NO₂) with a Copper Oxide Sensor Operated with a Pulsed Temperature Modulation

[1] **Aymen SENDI,** [1] **Grérory BESNARD,** [1] **Philippe MENINI,**
[1] **Chaabane TALHI,** [1] **Frédéric BLANC,** [1] **Bernard FRANC,**
[2] **Myrtil KAHAN,** [2] **Katia FAJERWERG and** [2] **Pierre FAU**

[1] LAAS-CNRS, University of Toulouse, CNRS, 7 Avenue du Colonel Roche, 31000 Toulouse, France
[2] LCC-CNRS, University of Toulouse, CNRS, 205 Route de Narbonne, 31000 Toulouse, France
[1] Tel.: +33.5.61.33.62.18, fax: +33.5.61.33.62.08
E-mail: sendi@laas.fr, besnard@laas.fr, menini@laas.fr, talhi@laas.fr, blanc@laas.fr, franc@laas.fr,
myrtil.kahn@lcc-toulouse.fr, katia.fajerwerg@lcc-toulouse.fr, pierre.fau@lcc-toulouse.fr

Abstract: NO₂ is considered among the main pollutants found in atmosphere and indoor air as well. The exposure to this gas is dangerous to human health; its detection is an urgent need that requires the development of efficient and cheap methods and techniques for detection and data processing. In this context, copper oxide is a good candidate metal oxide that is sensitive and selective for NO₂ at sub-ppm concentrations. We used a CuO composed by nanoparticles deposited by inkjet printing technology on a micro hotplate. The optimum detection capacity is obtained thanks to a dedicated temperature modulation. Thanks to this operating mode, we report a simple method for data processing and exploitation in order to obtain a good selectivity for the nitrogen dioxide over few interferent gases. Only four parameters get from sensor response allow us to make an efficient discrimination between individual gases but also in gaseous mixtures in humid atmosphere.

Keywords: NO₂, CuO nanoparticles, Temperature modulation, Gas sensor, Selectivity.

1. Introduction

Humans spend more than 90 % of their time in closed environments, even though this indoor environment offers a wide variety of pollutants [1-2]. Indoor air pollution is a real health threat, so measuring indoor air quality is important for protecting the health from chemical and gaseous contaminants. Nitrogen dioxide (NO₂) is a dangerous pulmonary irritant [1]. NO₂ is generated by multiple sources of combustion in indoor air, such as smoking and heaters, but it also comes from outside air (industrial sources, road traffic) [3]. NO₂ may have

adverse effects of shortness of breath, asthma attacks and bronchial obstructions [4].
It is also classified as toxic by the "International Agency for Research on Cancer (IARC)" [5], hence the necessity for sensor development for accurate NO₂ detection is an acute need. Among sensors techniques, the metal oxide gas (MOX) sensors are promising candidates because of their high performance in terms of sensitivity on top of their low production cost. The copper oxide (CuO) material is highly studied because of its high sensitivity and its ability to detect oxidant gaseous compounds, but also for other indoor air pollutants, such as acetaldehyde (C₂H₄O),

formaldehyde (CH_2O), NO_2, CO, etc. However, CuO (as well as other metal oxides) suffers from a major disadvantage which is the lack of selectivity with respect to targeted gas.

In this study, our main objective is to develop an innovative and simple pulsed- temperature operating mode associated with an efficient data processing technique, which enables good selectivity toward NO_2 in gas mixtures (combination of two gases). This technique is based on few parameters extracted from the dynamic response of sensor versus temperature changes in a gaseous environment. These parameters are: the normalized sensing resistance, the initial slope, the intermediate slope and the final slope of the response of NO_2 against different reference gases, such as C_2H_4O, CH_2O and moist air.

These four parameters allow us to follow the synthetic evolution of the adsorption phenomenon of gaseous molecules in the surface of the metal oxide during the gas injection. This synthetic evolution is different for each gas which allows us to define detection meanings for each gas in the range of the defined concentration. This technique greatly facilitates the discrimination of NO_2 toward other referent gas and improves the selectivity of CuO under different gas contaminant and condition in indoor air.

The selectivity of NO_2 was examined in relation to air moisture with 30 % humidity, C_2H_4O at 500-ppb, CH_2O at a concentration of 500-ppb and the binary mixture of these gases with 300-ppb of each.

In Section 2 of the paper, we describe the materials and methods used in our work. The Section 3 presents our results and the discussion. We conclude this work in Section 4.

2. Materials and Methods

2.1. Description of the Metal Oxide: the Copper Oxide

CuO nanoparticles have been obtained by the reaction of ambient air during 24 hours on copper acetamidinate precursor (Cu_{amd}) in the presence of 5 molar equivalents of octylamine (OA). [6] Excess of OA in the medium is removed by several precipitation stages by centrifugation and washing with THF. In Fig. 1 we show a SEM micrographic of a CuO.

The sensitive layer made of CuO nanoparticles is deposited by inkjet [7] printing on a silicon microhotplate [8] presented with more detail in the next section. We chose this technique because it is well adapted for various material integration on multisensor platform (our final goal) without additional photolithographies Moreover, it has been less studied toward the other deposit technique [9]. The ink is prepared with 5 % CuO weight, which was dispersed in ethylene glycol by an ultrasonic bath for about one hour. The dispersions obtained were allowed to settle for 24 hours. The final ink was collected and then used for printing using Altadrop equipment, where the numbers of the deposited drops

of ink were controlled [8]. The principle of operation of this device and the control of the number of drop is described in Fig. 2.
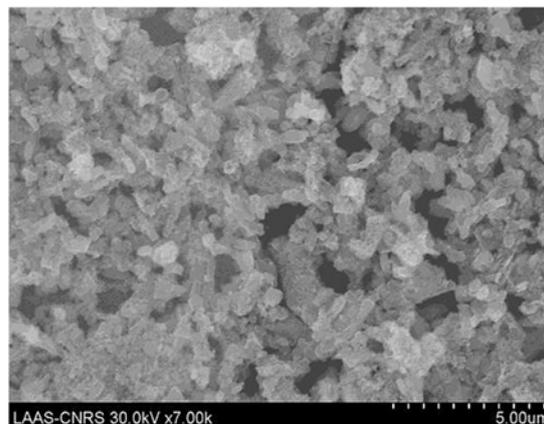

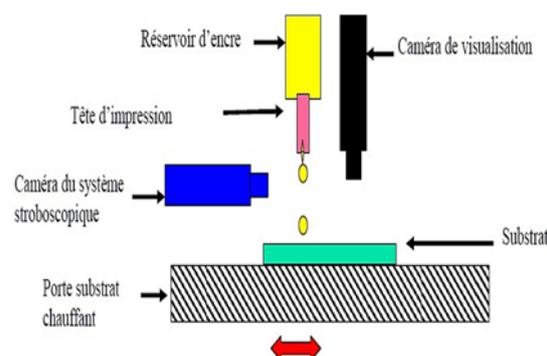**Fig. 1.** SEM micrographic of a CuO.

Fig. 2. Schematic diagram of the inkjet machine.

This technique is simple and allowed us to obtain reproducible thicknesses from one to a few micrometers depending on the number of deposited drops. In addition, this technique permits to have a precisely localized deposit without need of additional complex photolithographic steps. The CuO layer is finally deposited on the microhotplate and annealed in ambient air from room temperature to 500 °C (rate 1°C/min) followed by a plateau at 500 °C for 1 hour before cooling to room temperature (1°C/min). This initial temperature treatment is necessary because CuO requires operating temperatures between 100 °C<T<500 °C. The thermal pretreatment is necessary to generate ionized oxygen species in atomic or molecular form at the oxide surface and therefore to improve the reactivity between the reacting gas and the sensor surface [6].

2.2. Microhotplate

The microhotplate has been designed in the technology center of LAAS-CNRS in Toulouse in France, and optimized to increase the temperature up to 600 °C with low energy consumption (only 60 mW), a good reliability and high robustness [10].

This microhotplate is designed on a silicon mass present a support for a bilayer membrane composed by $SiO_2/SiNx$ on which the heater and the sensitive electrode are placed. The metallization of these electrodes is composed by a bilayer Ti/Pt then insulated by a SiO_2 passivation layer. In Fig. 3 we see a top view and a cross sectional view with different physical layer.
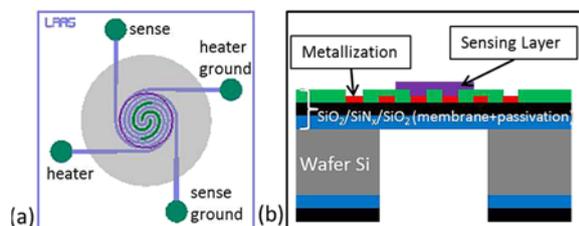

Fig. 3. Micro-hotplate gas sensor: (a) Top view, (b) Cross sectional view.

2.3. Operating Mode

In this study, we have used a pulsed temperature profile, which showed that optimized sensitivity can be achieved with the use of two different temperature stages at 100°C and 500°C respectively. This dual temperature protocol also reduces the total power consumption of the device (see Fig. 4).
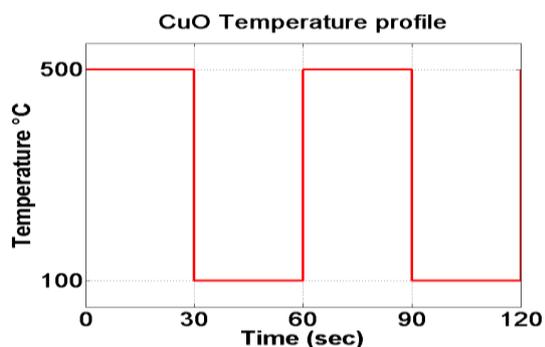

Fig. 4. CuO temperature profile.

This optimal profile was obtained thanks to a specific study on the during of each step and a different temperature modulation forms in order to obtain the best sensitivity of the copper oxide under NO_2. In this study we launched four tests by changing the duration of the step for each test and injected a 300-ppm of NO_2 to see where we can obtain the better sensitivity:

1- 1th test: with time step equal 2 seconds,
2- 2^{sd} test: with time step equal 10 seconds,
3- 3th test: with time step equal 30 seconds,
4- 4th test: with time step equal 60 seconds.

For each test we applied a temperature profile with two modulation forms:

- Pulsed down temperature modulation with a return to 500 °C after each pulse by applying on the

heater successively the following temperature: 500 - 400 - 500 - 300 - 500 - 200 and 500 – 100 °C.

- Descending step temperature modulation by applying on the heater successively the following temperature: 500 - 400 - 300 - 200 and 100 °C. (See Fig. 5).
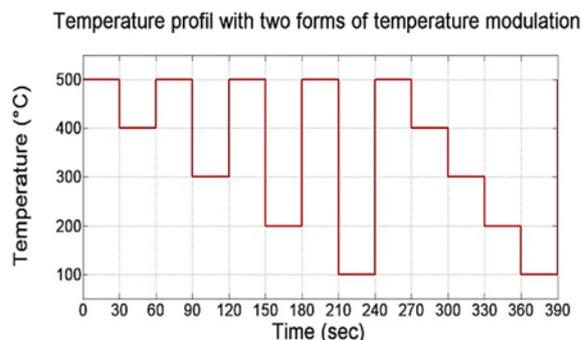

Fig. 5. Form of temperature modulation.

In all these tests we applied these two forms of modulation in the same profile in order to see the effect of the transition from a high temperature to a low temperature on the CuO sensitivity, passing through intermediary temperature without return to the step of the high temperature (in the case of pulsed down temperature modulation) and with a return towards this level in order to see the effect of heating the CuO follows a low temperature step on the gas detection. In Fig. 6 we show the results of these four tests.

Each bar shows the results of the normalized resistance of a gas injection for each time step by applying on the heater the temperature profile presented above.
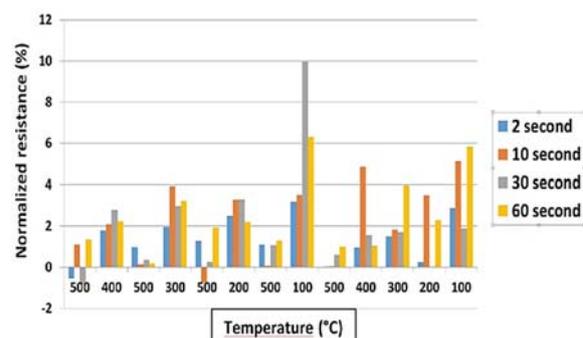

Fig. 6. Representation of the normalized resistance of CuO sensor under 300 ppb of NO_2 at different temperature stages.

By comparing the sensitivity bars and the transient responses during each temperature step, we concluded that the best performances under NO_2 was obtained with the pulsed down temperature modulation form and with a 30 seconds duration step. The transition that carry out the best sensitivity is from the highest temperature (500 °C) to the lower temperature

(100 °C) (grey color bar in Fig. 6), that explains our choice for the final temperature profile applied on our CuO sensor. CuO needs a high temperature at 500 °C for cleaning the surface of the metal oxide and a low temperature at 100 °C for measuring the adsorption under gas. In this way we obtained the optimal temperature profile for the CuO presented in Fig. 4.

This profile has then be applied on the heater of our CuO sensor for all further tests.

2.4. Material and Methodology

The CuO sensor was placed in a 250 ml test chamber and the test conditions were as follow:
- A flow rate of 200 ml/min, controlled by a digital flowmeter.
- A relative humidity (RH) level of 30 % is obtained by bubbling synthetic air flow controlled by a mass flow controller.
- The measuring chamber is at ambient temperature, controlled by a temperature sensor placed inside the vessel.
- A bias current is applied to the sensitive layer, controlled by a Source Measure Unit (SMU).

We started a test with single gas injections after a phase of two-hours stabilization in humid air, then with injections of binary mixtures for 16-min. During 32-min, moist air is injected between two successive gas injections. This time is enough to clean the chamber and stabilize the sensor to its baseline.

The gas injections concentrations are summarized in Table 1.

Table 1. Injected gases concentrations [11].

Gas	Concentration
Acetaldehyde (C_2H_4O)	0.5-ppm
Formaldehyde (CH_2O)	0.5-ppm
Nitrogen dioxide (NO_2)	0.5-ppm
Acetaldehyde and Formaldehyde (C_2H_4O/ CH_2O)	0.3-ppm/0.3-ppm
Acetaldehyde and Nitrogen dioxide (C_2H_2O/ NO_2)	0.3-ppm/0.3-ppm
Formaldehyde and Nitrogen dioxide (CH_2O/ NO_2)	0.3-ppm/0.3-ppm

A schematic representation of these injections is presented in Fig. 7.

During all the experience (stabilization phase, gases injections and stage between two successive gases), the sensor is powered by a square signal voltage applied on the heater in order to obtain two temperature steps as shown in Fig. 4. To ensure a constant overall flow, we adapted the gas injection sequences duration in correlation with the heating signal period (see Fig. 8).

The resistance variation of CuO is measured under a fixed supply current of 100 nA in order to obtain voltage measurements in the range of few volts, far

from compliance limit of the measuring device (20 V). We also verified that this procedure (temperature cycling) doesn't affect the sensor reproducibility in terms of baseline or the sensor sensitivity.
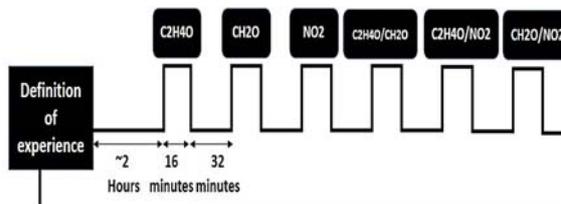

Fig. 7. Synoptic representative of a sequence of gas injections [11].
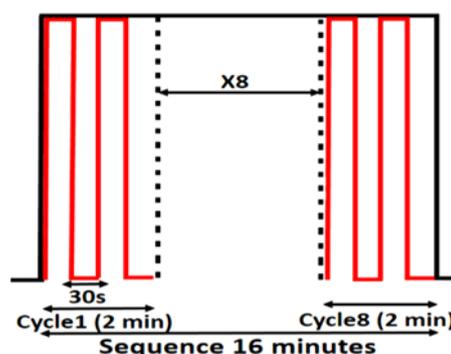

Fig. 8. Diagram of a gas sequence [11].

Under such test conditions, we achieved a continuous 6.5 hours testing period without observing any drift on the raw sensor response. The sampling period is 500 ms, which gives us 60 points on a 30-second response step, this acquisition rate being enough for accurate data processing [11].

Finally, we analyzed the sensor responses on each steps, according to the different gas injections, using a simple method of data processing in order to have the better selectivity of NO_2.

3. Results and Discussion

3.1. Method of Analysis

During each gas injection, 16 periods of temperature modulation are applied. After verifying the reproducibility of sensor responses along these cycles, we only present here the responses of the last cycle, which is stabilized and reproducible from one cycle to another. As mentioned previously, we used new simple data treatment methods to obtain the better selectivity toward NO_2 with respect to several interferent gases.

Among the multiple possible criteria, we chose representative variables that take into account the dynamic sensor behavior during a change of gaseous conditions and during a pulsed temperature; these

criteria are obtained from the sensor resistance slopes during the gas response on each 30-second-steps. The data acquisition relies on the decomposition of the response into three distinct domains in order to follow the synthetic evolution of CuO toward the different gas injections (see Fig. 9).

These domains are:

- Starting Slope: from the 1st point to the 10th point (in yellow).

- Intermediate slope: from the 10th point to the 30th point (in red).

- Final slope: from the 30th point to the 60th point (in black).

The normalized resistance is measured from the last point on each step: this is the absolute difference between the resistance of the sensor under a reference gas (like moist air) and the resistance of the sensor under targeted gas(es), at the final cycle of each injection:

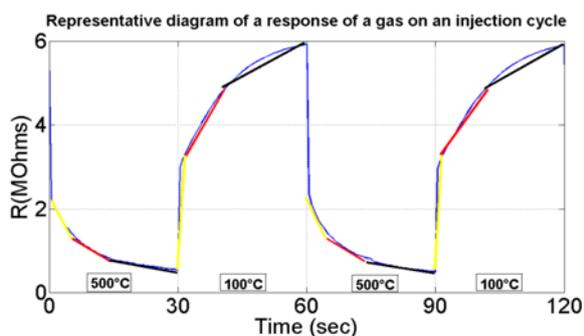$$Rn = \left(\frac{Rgas - Rair}{Rair}\right) * 100 \qquad (1)$$

Fig. 9. Representative diagram of a response of a gas sensor during an injection cycle and showing the 3 domain slopes [11].

By treating these four parameters, a good selectivity of NO_2 can be obtained with respect to moist air, C_2H_4O and CH_2O.

3.2. Results

Before starting the data treatment from each slope, we have based on the raw data and the graph of the gas injection responses. Fig. 10 shows the graph of the last cycle of a gas injection with the four temperature steps present the temperature profile applied. It is clear from this graph that the initial, the intermediate and the final slope at 500 °C are flat and near to zero (see Fig. 10).

In the next we treat the three domains one by one.

3.2.1. Initial Slope

The slope at the origin is calculated on the first 10 points of each temperature step of the 8th cycle of

each injection. Regarding the reference gas (moist air); we took the response of the 8th cycle of the last sequence under humid air before the injection of gases. The values of these slopes (in Ohms/ms) are shown in Fig. 11; each bar represents the value of the slope at the origin of each gas at 500 and 100 °C.
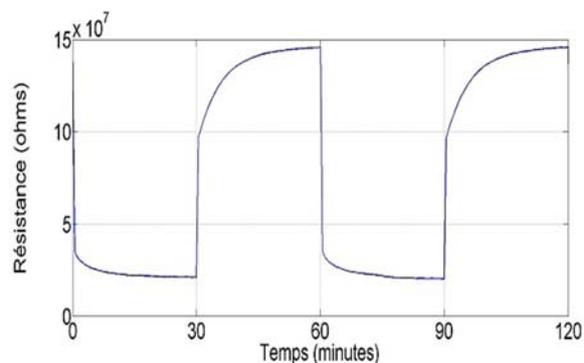

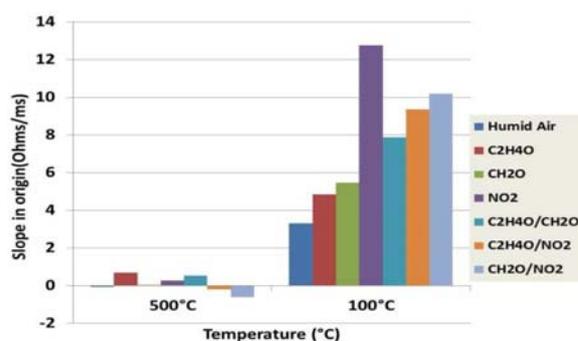**Fig. 10.** Example of a raw response gas injection.

Fig. 11. Representation of the slopes at the origin under different gases of the 8th cycle in "Ohms/ms" according to the temperature of the sensors [11].

The Fig. 11, clearly shows that the calculations of this parameter enable us to differentiate NO_2 from the other reference gases by measures on the step at 100 °C. Regarding the other step at 500 °C we note that the response is almost zero, because the transition from a cold to a hot state decreases the detection sensitivity and therefore reduces the sensors resistance variations under gas. We also note that with this criterion we evidence a significant difference between the value of the starting slope under NO_2 compare to others under other gases and mixtures without NO_2 [11].

3.2.2. Intermediate Slope

The intermediate slope is calculated from the 10th point to the 30th point of each temperature step of the last cycle during each gas injection and compared with the value under air. The calculated values are shown in Fig. 12.

According to Fig. 12, the value of the intermediate slope of individual NO_2 injection or of the gas

mixtures in which there is NO_2, is not prominent compared with the other reference gases even on the plateau at 100°C. This parameter is less effective than the previous one to detect NO_2 in gas mixtures [11].
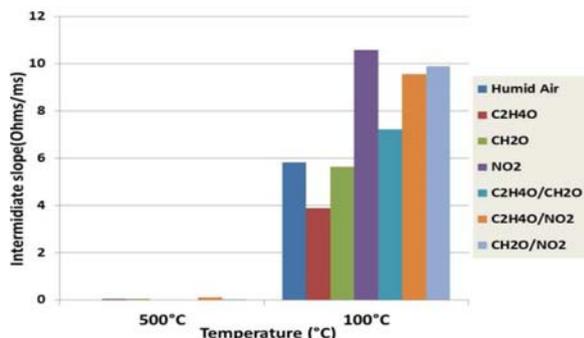

Fig. 12. Representation of the intermediate slopes under different gases at the 8th cycle in "Ohms/ms" according to the temperature of the sensors [11].

3.2.3. Final Slope

The final slope is the slope of the second half of the gas response; it is calculated between the 30th point and the 60th point. The response to the different temperature steps of the last cycle during NO_2 injection and the reference gases is presented in Fig. 13 [11].
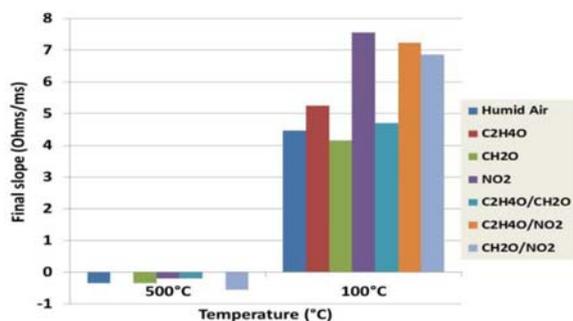

Fig. 13. Representation of the final slopes under different gases at the 8th cycle in "Ohms/ms" according to the temperature of the sensors [11].

It is worth noting that the value of the final slopes of NO_2 or gaseous mixtures, which contain the NO_2, are very different compared to the other reference gases on the two stages at 100°C only. This parameter allows us to select NO_2 with respect to other interfering gases.

3.2.4. Normalized Resistance

As previously presented, the normalized resistance is calculated with respect to humid air from each last cycle level. The reference resistance used is the resistance of each stage of the last wet air sequence before the gas injection. The results obtained from these calculations are shown in Fig. 14.
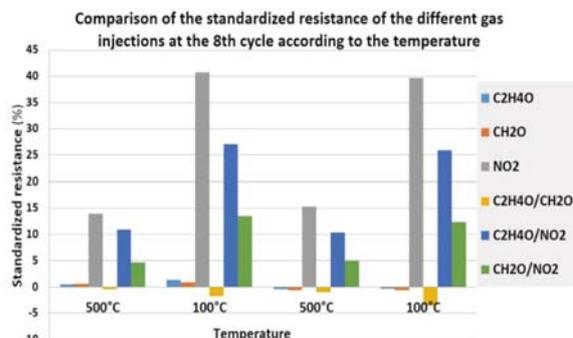

Fig. 14. The normalized resistance of the different gas injections at the 8th cycle according to the temperature [11].

The Fig. 14 shows a slight variation in the values of the normalized resistance between two similar and successive temperatures for the same gases. This slight variation can be explained by data dispersion which is +/- 2%, due to the fact that the normalized resistance is calculated from the raw values during the gas injection and the raw values of resistances during the injections of humid air that may be slightly different between two similar and successive temperature stages.

The CuO sensor response to sub-ppm NO_2 levels when injected individually or in combination with another gas, is specific when measurements are taken on the low temperature plateau at 100°C [11].

4. Conclusions

The selectivity and sensitivity of our CuO sensor has been studied by different operating modes and simple methods of analysis. Specific temperature modulation was applied to the metal oxide with the use of temperature steps at 500 and 100°C. The response of CuO sensitive layer toward gases representatives of indoor air pollution (C_2H_4O, CH_2O, NO_2, humid air) has been studied. These responses were analyzed with several parameters, such as the study of the slope of resistance variation at the origin, the intermediate slope, the final slope and the normalized resistance measured at each temperature steps. By using these 4 parameters we can to define a new PCA, different from what exists in the literature of gas sensors (PCA with only the study of standardized resistance). The effect of adding new elements to the raw data processing of a response improves the selectivity of the detected gases.

The study of these different parameters shows that the CuO material is able to detect sub-ppm levels of NO_2 with a good selectivity compared to different interfering gases. This study shows new parameters applicable to the PCA on any metal oxide in order to improve its selectivity.

To still improve the selectivity of gas sensor device to a larger variety of polluting gases, we plan to integrate these CuO sensors in a multichip system, which will allow us to use in parallel new metal oxide layers with specific temperature profiles and data analysis criteria.

Acknowledgments

References

[1]. B. Lévesque, P.-L. Auger, J. Bourbeau, J.-F. Duchesne, P. Lajoie, D. Menzies, Indoor air quality, *Environment and Public Health. Foundations and Practices*, 2003, pp. 317-332.

[2]. J. Namiesnik, T. Gorecki, B. Kozdron-Zabiega, J. Lukasiak, Indoor air quality (IAQ), pollutants, their sources, and concentration levels, *Building and Environment,* Vol. 27, Issue 3, 1992, pp. 339-356.

[3]. Roger Cadiergues, Indoor air quality (IAQ), *Guide/Ref CAD*: nR15.a., 2017, pp. 16-17.

[4]. K. Koistinen, D. Kotzias, S. Kephalopoulos, C. Schlitt, P. Carrer, M. Jantunen, S. Kirchner, J. McLaughlin, L. Molhave, E. Fernandes, B. Seifert, The INDEX project: Executive summary of a European Union project on indoor air pollutants, *Allergy*, Vol. 63, Issue 7, 2008, pp. 810-819.

[5]. D. Loomis, W. Huang, G. Chen, The International Agency for Research on Cancer (IARC). Evaluation of the carcinogenicity of outdoor air pollution: focus on China, *Chin J Cancer.*, Vol. 33, Issue 4, 2014, pp. 189-196.

[6]. J. Jońca, A. Ryzhikov, S. Palussière, J. Esvan, K. Fajerwerg, P. Menini, M. L. Kahn, P. Fau, Organometallic synthesis of CuO nanoparticles: Application in low temperature CO detection, *ChemPhysChem*, Vol. 18, Issue 19, 2017, pp. 2658-2665.

[7]. M. Morozava, P. Kluson, J. Krysa, P. Dzik, M. Vesely, O. Solcova, Thin TiO_2 films prepared inkjet printing of the reverse micelles sol-gel composition, *Sensors and Actuators B: Chemical*, Vol. 160, 2011, pp. 371-378.

[8]. N. Dufour, A. Chapelle, F. Mesnilgrente, V. Conedera, Ph. Menini, Technological improvements of a metal oxide gas multi-sensor based on a micro-hotplate structure and inkjet deposition for an automotive air quality sensor application, in *Proceedings of the 25th Micromechanics and Microsystems Europe Workshop (MME 2014),* Istanbul, Turkey, Aug. 2014, pp. 1-5.

[9]. J. Kukkola, E. Jansson, A. Popov, J. Lappalainen, J. Mäklin, N. Halonen, G. Tóth, A. Shchukarev, J.-P. Mikkola, H. Jantunen, K. Kordás, J. Hast, T. Hassinen, A. Sunnari, K. Jokinen, H. Haverinen, R. Sliz, G. Jabbour, T. Fabritiuc, R. Myllylä, A. Vasiliev, N. Zaretskiy, Novel printed nanostructured gas sensors, *Procedia Engineering*, Vol. 25, 2011, pp. 896-899.

[10] P. Yoboue, A. Konaté, O. Asseu, P. Tety, P. Ménini, An Industrializable silicon based microhotplate for metal oxide gas sensors, *International Journal of Physical and Chemical News (PCN journal)*, Vol. 72, 2014, pp. 34-41.

[11]. A. Sendi, G. Besnard, Ph. Menini, Ch. Talhi, F. Blanc, B. Franc, M. Kahn, K. Fajerwerg, P. Fau, Sub-ppm Nitrogen Dioxide (NO2) Sensor Based on Inkjet Printed CuO on Microhotplate with a Pulsed Temperature Modulation, in *Proceedings of the Third International Conference on Advances in Sensors, Actuators, Metering and Sensing (ALLSENSORS 2018)*, Rome, Italy, 24-29 March 2018.